Benchmarking Electronic Structure Calculations on the Bare UO_2^{2+} Ion: How Different are Single and Multireference Electron Correlation Methods?†

Florent Réal,‡ André Severo Pereira Gomes,§ Lucas Visscher,§ Valérie Vallet,*,‡ and Ephraim Eliav||

Université Lille1 (Sciences et Technologies), Laboratoire PhLAM, CNRS UMR 8523, CERLA, CNRS FR 2416, Bât P5, F-59655 Villeneuve d'Ascq Cedex, France, Amsterdam Center for Multiscale Modeling, Department of Theoretical Chemistry, Faculty of Sciences, Vrije Universiteit Amsterdam, De Boelelaan 1083, 1081 HV Amsterdam, The Netherlands, and School of Chemistry, Tel Aviv University, 69978 Tel Aviv, Israel

Received: April 23, 2009; Revised Manuscript Received: June 15, 2009

In a recent investigation by some of us on the spectrum of the uranyl (UO_2^{2+}) ion [Réal, F.; Vallet, V.; Marian, C.; Wahlgren, U. *J. Chem. Phys.* **2007**, *126*, 214302], a sizable difference between CASPT2 and linear response coupled cluster (LRCC) was observed both with and without the perturbative inclusion of spin−orbit coupling. This poses a serious question as to which of the two would be more reliable for investigating molecules containing actinides. In this paper we address this question by comparing CASPT2 and LRCC to a method known to accurately describe the spectra of actinide-containing molecules: the four-component intermediate Hamiltonian Fock-space coupled cluster (IHFSCC) method, where electron correlation and spin−orbit coupling are treated on an equal footing. Our results indicate that for UO_2^{2+} there is little difference between treatments of spin−orbit coupling, making electron correlation the main cause of discrepancies. We have found IHFSCC and LRCC to be the most alike in the overall description of excited states, even though individual LRCC energies are blue-shifted in comparison to IHFSCC due to the difference in the parametrization of the excited states' wave functions. CASPT2, on the other hand, shows good agreement with IHFSCC for individual frequencies but significantly less so for the spectrum as a whole, due to the difference in the degree of correlation recovered in both cases.

1. Introduction

The chemistry of actinide-containing molecules is a rich and fascinating subject, in particular because of their spectroscopic and luminescence properties. The luminescence of uranyl(VI) UO_2^{2+} has been extensively studied experimentally both in aqueous solution and in crystals. However, the assignment of the energy levels responsible for the strong absorption in the UV range and the long-lived luminescent state that emits light in the visible (20 000−26 000 cm^{-1}) range is not trivial.[1−3] There have been several theoretical studies in the past decade on the electronic spectrum of uranyl(VI), either as a bare ion[4−7] or coordinated[5,6,8,9] to other species, with the 2-fold aim of comparing theoretical methods and reproducing the experimental data available in the condensed phase. Theoretical approaches face several challenges due to the large number of electrons, which should be treated explicitly, and to the accurate description of the strong interactions of the uranyl with its surroundings (ligands, host crystals, or solvent molecules). Due to these interactions, unambiguous comparison between theoretical and experimental data is often difficult, and it is of interest to obtain benchmark theoretical data for the bare uranyl ion for which no experimental data is available.

In order to reach benchmark accuracy different hierarchies of methods could be applied: one can start from a relativistic framework, either via four-component[10,11] or two-component[12,13] treatments, in which spin−orbit is included a priori, and use multireference coupled-cluster[14−17] or configuration interaction (CI) methods[18−21] to treat electron correlation effects. An alternative is to use a two-step approach. In the first step, the correlation effect on the states of interest is treated at the spin-free (SF) level with CI-based methods such as multireference MRCI[22] or complete active space with second-order perturbation theory CASPT2[23−25] approaches, or by applying coupled cluster theory in the framework of response theory.[26−29] In the second step of the calculation, spin−orbit interaction between the various spin-free states is accounted for by performing spin−orbit configuration interaction (SOCI) calculations.[25,30] The effect of electron correlation computed in the first step is taken into account by means of an effective Bloch Hamiltonian.[31] The diagonalization of the total Hamiltonian yields energies and eigenvectors which take into account both correlation and spin−orbit effects. All of these methods are rather demanding and are often replaced by methods that reduce the work in either the treatment of electron correlation, such as time-dependent density functional theory (TDDFT), or in the treatment of relativity, e.g., using pseudopotentials, or both. Most approximate correlation schemes lack however, the possibility of systematically improving the description by going to the next level in a well-defined hierarchy.

In recent theoretical studies on the uranyl(VI) spectrum[7,9,32] several theoretical methods have been compared. Within the TD-DFT scheme, most density functionals do not yield accurate excitation energies; however, geometries and relaxation energies of the excited states are in most cases reasonably well described. Réal and co-workers[7] also demonstrated that different wave function-based methods generally provide qualitatively similar

† Part of the "Russell M. Pitzer Festschrift".

* To whom correspondence should be addressed. E-mail: valerie.vallet@univ-lille1.fr.

‡ CNRS UMR 8523.

§ Vrije Universiteit Amsterdam.

|| Tel Aviv University.

10.1021/jp903758c CCC: $40.75
Published on Web 07/16/2009

results. However, in quantitative terms significant differences appear between the two methods expected to yield the most accurate results: CASPT2 and linear response coupled cluster (LRCC). The LRCC spectrum was blue-shifted in comparison with that of CASPT2 by about 3000 cm^{-1} and quite similar to spectra obtained from multireference CI (MRCI) or averaged-quadratic coupled-cluster (AQCC) calculations. The only experimental spectra available are for crystals such as Cs_2UO2Cl_4[3] or in solution.[33] Matsika and Pitzer[5] and Pierloot et al.[6,9] have shown that the environment (the equatorial ligands and the rest of the crystal) may modify the character of the excited states, apart from changing significantly the transition energies. This greatly reduces the usefulness of comparing calculated energy levels for the bare uranyl to experimental values.

The need for understanding the origin of the discrepancies among wave function based methods in the computed uranyl energy levels has motivated us to employ the intermediate Hamiltonian Fock space coupled cluster (IHFSCC) method, a true multireference coupled cluster method that, in its relativistic formulation,[14−16] allows us to consider spin−orbit coupling and electron correlation on the same footing. The accuracy of the relativistic IHFSCC approach has been demonstrated in several investigations on actinyl species.[34−37] Moreover, Fock-space coupled cluster provides an ideal measure for the relative accuracy and reliability of both LRCC and CASPT2 because it is fully size-extensive for both ground and excited states (as opposed to LRCC, which is formally so only for the ground state) and includes electron correlation to infinite order (as opposed to CASPT2, which does so to second order). By providing a comparison of LRCC and CASPT2 to the accurate IHFSCC, we complement the picture obtained from previous studies, since the former have been compared extensively to more approximate wave function-based methods (e.g., MRCI and AQCC) and TD-DFT.[7,9,32]

2. Computational Details

2.1. Fock-Space Coupled Cluster. The calculations of the excitation spectrum of UO_2^{2+} were performed with a development version of the Dirac08 program,[38] using three different approaches to treat relativity. In the spin-free Dirac−Coulomb (SFDC)[11,39] calculations, we eliminate all spin−orbit coupling terms to allow for straightforward comparison with earlier works. This approach is an approximation to the regular 4-component Dirac−Coulomb (DC) calculation, in which only the usual approximation of (SS|SS) integrals by an a posteriori correction[40] is applied. The third approach concerns the eXact 2-Component (X2C) approach recently introduced by Iliaš and Saue[13] in which spin−orbit coupling is included from the start via atomic mean-field integrals calculated with the AMFI code.[41,42]

In most of the calculations the valence double (DZ) or triple-ζ (TZ) basis sets by Dyall[43] were used for the uranium atom, but we also considered the Fægri set,[44] that corresponds to triple-ζ (TZ) quality in the valence s functions, and quadruple- ζ (QZ) or higher quality for the higher angular momenta. For oxygen we employed the (aug)-cc-VDZ and aug-cc-pVTZ basis sets of Dunning and co-workers.[45] All of these basis sets were kept uncontracted in all calculations.

The potential energy curves for the symmetric stretch were sampled at 14 different uranium−oxygen bond lengths (r_{UO}) within the range $r_{UO} \in [1.58;1.92]$ (Å). This ground-state potential energy curve was described by the Dirac−Coulomb coupled cluster single and double without (CCSD) and with perturbative treatment of triples (CCSD(T)) method,[46−49] while

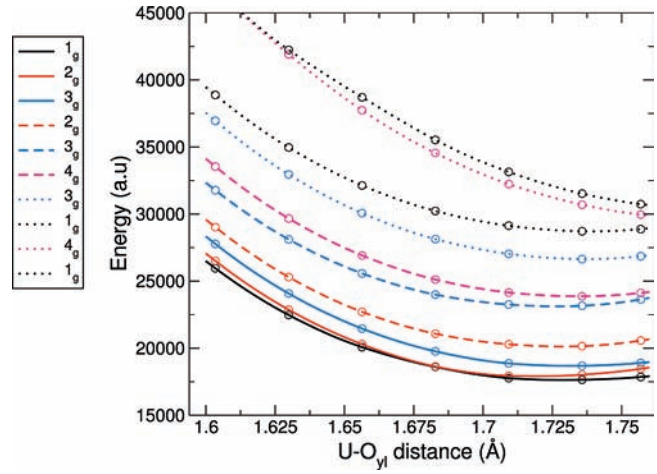

Figure 1. Potential curves of the uranyl (VI) bare ion along the symmetric stretching mode computed with the SO-IHFSCC method. The 1_g states are drawn in black, the 2_g in red, the 3_g in blue, and the 4_g in magenta.

the curves for the excited states were obtained within the IHFSCCSD scheme using the "one particle, one hole" sector (1*h*,1*p*) of Fock space. In the calculations, several active spaces were tested; only orbitals with orbital energies (in au) $\varepsilon \in [-6.00; 20.00]$ (34 electrons), $[-3.00; 20.00]$ (24 electrons; uranium 5d frozen), and $[-3.00; 40.00]$ (24 electrons; testing the effect of higher lying virtual orbitals) are included in the correlation treatment. These different active spaces will be referred to as AS1, AS2, and AS3, respectively.

In Fock-space coupled cluster calculations one should subdivide the space spanned by the active orbitals in two subspaces: the model or *P* space, containing the active valence orbitals which are directly involved in the electronic excitations and the complementary *Q* space that includes the remaining "correlation-active" orbitals from AS1, AS2 or AS3. In the present case this translates into including the highest occupied orbitals ($\sigma_{1/2u}$, $\sigma_{1/2g}$, $\pi_{1/2u}$, $\pi_{3/2u}$, $\pi_{1/2u}$ and $\pi_{3/2g}$) and the ten lowest unoccupied (the nonbonding uranium $f^{\delta}_{3/2u}$, $f^{\delta}_{5/2u}$ and $f^{\phi}_{5/2u}$, $f^{\phi}_{7/2u}$, as well as the antibonding $\sigma^*_{1/2u}$, $\sigma^*_{1/2g}$, $\pi^*_{1/2u}$, $\pi^*_{3/2u}$, $\pi^*_{1/2u}$ and $\pi^*_{3/2g}$) orbitals in the (*P*) model space. This space can be extended by considering in addition the deeper lying occupied orbitals (6s, 6p, and 5d on uranium and 2s on the oxygens) and/or higher virtual orbitals (see Figure 1 in ref 3 for a schematic spin-free picture on the composition of these orbitals).

The intermediate Hamiltonian facilitates such extensions of the active space by allowing for a further subdivision of the resulting model space into 2 subspaces, the main model (P_m) space and an intermediate model (P_i) space that is not dressed and serves as a buffer between the P_m and *Q* spaces, thus alleviating "intruder" state problems. The main model space P_m (consisting here of 14 electrons and 34 spinors for AS1, and of 12 electrons and 24 spinors for AS2 and AS3, respectively) is built solely from excitations within the subset of main active valence orbitals, whereas every configuration from the P_i subspace involves at least one intermediate active valence orbital.

One should realize that accurate solutions are only obtained for states dominated by P_m components. The undressed P_i space merely serves as a buffer to eliminate intruder state problems that make convergence in traditional Fock space approaches difficult. The scheme employed here is known in literature as IH2,[50,51] but for simplicity we refer to it simply as IHFSCC. This method forces the $P_i \rightarrow Q$ transition amplitudes of the wave

TABLE 1: Calculated U−O_{yl} Distances R_e (Å) and Harmonic Frequencies ω_e (cm^{-1}) Computed for Various Correlation Methods Including All Relativistic Effects

	4C				1C					
method	this work		de Jong et al.[a]		Straka et al.[b]		Réal et al.[c]		Pierloot et al.[d]	
ref.	R_e	ω_e	R_e	ω_e	R_e	ω_e	R_e	ω_e	R_e	ω_e
MP2	1.724	957	1.739	944	1.728	1053				
CCSD	1.685	1103	1.697	1041			1.679	1038		
CCSD(T)	1.703	1016	1.715	974	1.702	1111				
CASPT2									1.708	1103

[a] Reference 55a. [b] Spin-free values; ref 56. [c] Reference 7. [d] Reference 6.

function operator to be zero, which makes the scheme easy and efficient to use.[34,35]

2.2. Linear Response CCSD. Calculations with the linear response CCSD method[26−29] were made with the implementation available in the Dalton 2.0 package.[52] These were carried out to check the influence of uncontracting the basis sets in such calculations, in order to make the comparison of our current results and the previous spin-free LR-CCSD work (in which a contracted atomic natural orbital basis set was used) more straightforward. The Fægri basis set mentioned above was thereby used for uranium, along with the cc-pVTZ basis for oxygen. In this case molecular orbitals were obtained from a scalar relativistic Hartree−Fock calculation using the Douglas−Kroll−Hess Hamiltonian.[53,54] In the spin-free LR-CCSD calculation, the uranium atomic orbitals below the 6s were kept frozen as well as the 1s oxygen atomic orbitals, thus correlating 24 electrons. The highest virtual orbitals with energies $\varepsilon \geq 40$ au were discarded from the orbital correlation space.

2.3. Computational Requirements. Given this range of different methods employed in the current work it may be of interest to list some representative computational requirements for the calculations performed: the one-component correlated calculations can be performed on a typical Linux cluster with one processor and about 1 Gb memory, while the requirements of the four-component DC-IHFSCC go up to 4Gb memory (in solving the amplitude equations for the different sectors of the Fock space) and about 80 Gb of disk space (in the transformation from AO to MO basis, prior to the coupled cluster calculation) per processor, which are more easily met on a supercomputer.

3. Results and Discussion

3.1. Ground-State Spectroscopic Constants. The spectroscopic constants of the ground state of UO_2^{2+} already provide information on possible differences between the combinations of basis sets and Hamiltonians that we wish to compare. The bond lengths and vibrational frequencies computed with the (4C−)MP2, (4C−)CCSD and (4C−)CCSD(T) methods are reported in Table 1 and may be compared to those available in the literature.[6,7,55,56]

Our calculations yield U−O_{yl} bond lengths of 1.724, 1.685, and 1.703 Å for 4C-MP2, 4C−CCSD, and 4C−CCSD(T), respectively (from fitting 7 points near the respective minima with a 4th degree polynomial). It is clear that the inclusion of triple excitations in the coupled cluster allows for relaxation of the U−O_{yl} bonding orbitals, resulting in a slight bond lengthening (0.02 Å), while the bond distance is overestimated by 4C-MP2. These results are quite similar to those obtained by de Jong et al.[55] in previous four-component calculations with the differences of 0.012 Å between the two sets of results likely arising from the different basis sets used in both studies - those used here are more flexible than those used by de Jong et al.[55] The 4C-MP2 results are also quite similar to those obtained by Straka et al.[56] with a scalar relativistic MP2 calculation, as was expected since spin−orbit effects are known to be of little importance for the properties of the uranyl closed-shell ground state.[57,58]

The SO-CASPT2 bond lengths[6] are shorter by about 0.02 Å than the 4C-MP2 ones, while they differ by less than 0.005 Å from the 4C−CCSD(T) values. This is surprising at first glance as one might expect MP2 and CASPT2 to yield similar results for the uranyl ground state for which the wave function is dominated by a single closed-shell determinant.[59] Even so, the ground-state CAS wave function (with an active space including the six bonding, six antibonding orbitals and four nonbonding orbitals) computed in the one component framework includes a significant contribution (about 13%) from double excited determinants. This leads to higher order excitations in CASPT2, relative to the MP2 and a better description of electron correlation, thus bringing the result closer to CCSD(T) accuracy.

Vibrational frequencies for the ground state, computed in the harmonic approximation, are also given in Table 1. As was the case for the bond lengths, we see in general good agreement with the results of de Jong et al.,[55] with discrepancies of about 40 cm^{-1} for 4C−CCSD and 4C−CCSD(T) numbers, but only 13 cm^{-1} for the 4C-MP2 ones. The frequency values vary in accordance with the trend observed for the equilibrium bond distances: the larger the bond length, the smaller the frequency. The SO-LR-CCSD results of Réal et al.[7] differ by 65 cm^{-1} from the 4C−CCSD ones. Although the bond lengths computed by Straka et al.[56] agreed with the 4C-values within 0.001 Å, the stretching frequencies show discrepancies of about 100 cm^{-1}. Similarly, for SO-CASPT2 the equilibrium bond distance[9] are nearly identical to the 4C−CCSD(T) value, while the symmetric stretching frequency is larger by about 90 cm^{-1}. This could indicate that the methods differ somewhat in the description of the electron correlation along the internal coordinates, but we are uncertain as to what extent these differences are intrinsic to the methods or whether inaccuracies in the determination of the frequencies play a role. Our experience obtaining frequencies from polynomial fits near the minima for this system indicates that these are rather sensitive to the fitting procedure, and lack of information as to how these have been obtained in the previous works restricts our ability to test this dependence on the fit.

3.2. Comparison of Vertical Transitions Computed in Scalar Relativistic Calculations. We start our discussion of the excited state calculations by comparing results obtained without inclusion of spin−orbit coupling, to focus on the influence of the electron correlation treatment. Results from spin-free calculations are reported in Table 2. We first note that differences due to choice of basis set are small: the two sets of LR-CCSD transition energies differ by at most 1000 cm^{-1}. The differences due to the choice of correlation method are very significant, with LR-CCSD transition energies of both the *u* and

TABLE 2: Spin-Free Vertical Transitions Energies ΔE^0 (in cm^{-1}) of UO_2^{2+} Computed at the IHFSCCSD, LR-CCSD, and CASPT2 levels[a]

	IHFSCCSD[b]			LR-CCSD[b]		LR-CCSD[c]		CASPT2[d]	
state	character	ΔE^0	ΔE^1	ΔE^0	ΔE^1	ΔE^0	ΔE^1	ΔE^0	ΔE^1
$a^3\Delta_g$	$\sigma_u f_\delta$	20972		24378		24441		22477	
$a^3\Phi_g$	$\sigma_u f_\phi$	23050	(2078)	26461	(2083)	26154	(1713)	23689	(1212)
$a^1\Phi_g$	$\sigma_u f_\phi$	27545	(6573)	30975	(6598)	30936	(6495)	27966	(5489)
$a^1\Delta_g$	$\sigma_u f_\delta$	30177	(9205)	33911	(9534)	33927	(9486)	31437	(8960)
$a^1\Delta_u$	$\sigma_g f_\delta$	37876	(16904)	41555	(17178)	42100	(17659)	36644	(14167)
$a^3\Delta_u$	$\sigma_g f_\delta$	38339	(17367)	41664	(17287)	42234	(17793)	37283	(14806)
$a^1\Pi_g$	$\pi_u f_\delta$	38776	(17804)	*42137*	(17759)	*43098*	(18657)	*37733*	(15256)
$a^3\Pi_g$	$\pi_u f_\delta$	39029	(18057)	*41278*	(16900)	*42188*	(17747)	*37181*	(14704)
$a^3\Gamma_g$	$\pi_u f_\phi$	39611	(18639)	*42168*	(17790)	*42981*	(18540)	*37563*	(15086)
$a^3\Phi_u$	$\sigma_g f_\phi$	40059	(19087)	43368	(18991)	43728	(19287)	38016	(15539)
$a^1\Phi_u$	$\sigma_g f_\phi$	40632	(19660)	*44137*	(19759)	44487	(20046)	38248	(15771)
$a^1\Gamma_g$	$\pi_u f_\phi$	41435	(20463)	*43909*	(19532)	44686	(20245)	39172	(16695)
$a^1\Pi_u$	$\pi_g f_\delta$	46126	(25154)	*50479*	(26101)	*51417*	(26976)	*43192*	(20715)
$a^3\Pi_u$	$\pi_g f_\delta$	46134	(25162)	*48491*	(24113)	*49426*	(24985)	*42602*	(20125)
$b^1\Gamma_u$	$\pi_g f_\phi$	48442	(27470)	51293	(26915)	52022	(27581)	44314	(21837)
$b^3\Gamma_u$	$\pi_g f_\phi$	49144	(28172)	51127	(26749)	52222	(27781)	44784	(22307)

[a] The energy differences ΔE^1 with respect to the first excited state are reported in parentheses. Changes in the ordering of the states are marked in italics. [b] Uranium Fægri and oxygen cc-pVTZ basis sets; $R(U-O_{yl}) = 1.683$ Å. [c] Reference 7; uranium ANO-RCC-QZP and oxygen ANO-RCC-TZP basis sets; $R(U-O_{yl}) = 1.683$ Å. [d] Reference 6; uranium DK3 and oxygen ANO-L basis sets; $R(U-O_{yl}) = 1.708$ Å.

g states being about 3000−3500 cm^{-1} higher than the corresponding IHFSCC numbers (calculated in the same basis and at the same distance). Since the ground state of the UO_2^{2+} ion can be described by a single determinant, the correlation in the coupled cluster method is in principle equivalent in the spin-free 4C and 1C frameworks. Thus, the discrepancy must come from differences in the correlation treatment for the excited states; more precisely due to the differences between IHFSCC and LRCC. These differences, which arise from the parametrization of the excited states wave functions, have been addressed extensively by other authors in previous publications,[60−64] but usually for rather light molecules with relatively few valence electrons.

LRCC is based upon a linear parametrization in terms of the ground-state coupled-cluster wave function, corresponding to a wave operator $\Omega^{LRCC} = (1 + C_k)$ that, upon application to the ground-state coupled cluster reference wave function, yields the excited state wave functions

$$|\Psi_k^{LR}\rangle = \Omega^{LR}|CC\rangle = (1 + C_k)\exp(T)|\Phi_0\rangle \qquad (1)$$

The (IH)FSCC parametrization is based upon the exponential of the cluster operator *S*, with a wave operator that is written as

$$|\Psi_k^{FS}\rangle = \Omega^{FS}|\Phi_0\rangle = \exp(S)|\Phi_0\rangle = \exp(S')\exp(T)|\Phi_0\rangle \qquad (2)$$

where *S* has been subdivided into ground-state amplitudes *T* and separate cluster operators for each sector of the Fock space ($S' = S(1,0) + S(0,1) + S(1,1)$) under consideration. For ionization potentials and electron affinities, IHFSCC and LRCC methods are formally equivalent since the expansion of exp (*S*′) truncates on the linear term.[62,63]

For higher sectors such as the (1*h*,1*p*) used in this work, both methods yield different results, since Fock-space methods contain terms such as $S^{(0,1)}S^{(1,0)}$,[62,63] which cancel out the disconnected terms arising from the linear parametrization in Ω^{LRCC} to third order or higher.[60−63]

This feature makes Fock-space methods size-extensive for both ground and excited states,[63,64] and should be the main reason for the systematic difference of about 3000−3500 cm^{-1} in excitation energies between the two methods (compare the first and second column of Table 2). Recent numerical comparisons between Fock-space and LRCC approaches by Musial and Bartlett,[65−67] are in qualitative agreement with our results, with LRCC yielding higher excitation energies than IHFSCC. In general the differences observed in the molecules considered then (N_2, H_2O, CO) are smaller than the ones computed here, which could be due to the larger number of electrons contributing to the correlation energy differences in UO_2^{2+}.

Comparison between the coupled cluster methods and the CASPT2 approach is less straightforward, as both methods already differ in the parametrization of the ground-state wave function. This is evident from the results discussed in the previous section and poses the question how best to compare vertical excitation energies. We have thereby chosen to present energies computed at a near-optimal bond length for each method.

Comparing the first and last column of Table 2, we see that the CASPT2 energies in most cases overestimate the excitation energies relative to IHFSCC, but in contrast to the systematic shift found with LR-CCSD, we also find some transitions computed up to a few thousand cm^{-1} lower than with IHFSCC.

The individual CASPT2 energies, particularly for the lower excited states (up to about 38 000 cm^{-1}), are in rather good agreement with IHFSCC ones, but this agreement deteriorates as higher states are considered. In the IHFSCC calculations the excited states below 41 000 cm^{-1} are dominated (>95%) by determinants within the P_m space and excitation energies should therefore be reliable. Above 41 000 cm^{-1}, contributions from determinants in the P_i space start to be more significant in particular for some Π states (such as the $a\ ^1\Pi_u$ at 46126 cm^{-1}), making the accuracy less certain and suggesting that discrepancies with CASPT2 could also arise from the inclusion of inaccurate "undressed" states in the IHFSCC calculation, even though our model space is larger than the largest CAS (12 electrons in 16 orbitals).

Apart from comparing the excitation energies directly, it is interesting here to analyze the energy differences between

TABLE 3: SO-IHFSCC Vertical Excitation Energies (in cm^{-1}) of UO_2^{2+} with Different Active Spaces, Hamiltonians and Basis Sets. The Energy Range of the Selected Orbitals in the CCSD Part Is between −3 au and 20 au, Except when the 5d Shell Is Correlated then the Lower Value Is about −7 au. Changes in the Ordering of the States Are Marked in Italics

basis U	Dyall DZ				Dyall DZ			Dyall TZ	Fægri TZ		
basis O	aug-cc-pVDZ				aug-cc-pVTZ			aug-cc-pVTZ	cc-pVTZ		
5d		frozen	in Q	in P_i	frozen			frozen	frozen		
state	Ω	X2C			Ω	X2C	4C-DC	4C-DC	Ω	4C-DC	composition (wrt. *h*–*p* determinants)
1	2_g	18777	18536	18571	1_g	18789	18984	18506	1_g	18610	81% $\sigma_{1/2u}f^{\delta}_{3/2u}$ + 15% $\pi_{1/2u}f^{\delta}_{3/2u}$
2	1_g	18949	18555	18591	2_g	18871	19065	18529	2_g	18633	69% $\sigma_{1/2u}f^{\phi}_{5/2u}$ + 13% $\sigma_{1/2u}f^{\delta}_{3/2u}$ + 11% $\pi_{1/2u}f^{\phi}_{5/2u}$
3	3_g	20128	19726	19760	3_g	20042	20233	19662	3_g	19765	75% $\sigma_{1/2u}f^{\phi}_{5/2u}$ + 13% $\pi_{1/2u}f^{\phi}_{5/2u}$
4	2_g	21411	21093	21127	2_g	21348	21536	20987	2_g	21080	45% $\sigma_{1/2u}f^{\delta}_{3/2u}$ + 22% $\sigma_{1/2u}f^{\delta}_{5/2u}$ + 16% $\sigma_{1/2u}f^{\phi}_{5/2u}$
5	3_g	24368	24202	24233	3_g	24310	24496	23914	3_g	23996	73% $\sigma_{1/2u}f^{\delta}_{5/2u}$ + 12% $\pi_{1/2u}f^{\delta}_{5/2u}$ + 7% $\sigma_{1/2u}f^{\phi}_{7/2u}$
6	4_g	25668	25388	25417	4_g	25509	25688	25049	4_g	25117	83% $\sigma_{1/2u}f^{\phi}_{7/2u}$ + 15% $\pi_{1/2u}f^{\phi}_{7/2u}$
7	3_g	28784	28531	28557	3_g	28629	28795	28066	3_g	28132	73% $\sigma_{1/2u}f^{\phi}_{7/2u}$ + 10% $\pi_{1/2u}f^{\phi}_{7/2u}$ + 8% $\sigma_{1/2u}f^{\phi}_{5/2u}$
8	2_g	30594	30425	28557	2_g	30694	30861	30177	2_g	30230	56% $\sigma_{1/2u}f^{\delta}_{5/2u}$ + 24% $\sigma_{1/2u}f^{\delta}_{3/2u}$ + 10% $\pi_{1/2u}f^{\delta}_{5/2u}$
9	0_g^-	32121	32132	32124	1_g	35216	35423	34544	1_g	34556	95% $\pi_{3/2u}f^{\phi}_{5/2u}$
10	0_g^+	32384	*32391*	*32382*	4_g	36214	36417	35495	4_g	35528	97% $\pi_{3/2u}f^{\phi}_{5/2u}$
11	1_g	33222	*33221*	*33211*	0_g^-	36415	36602	*35909*	0_g^-	35840	92% $\pi_{3/2u}f^{\delta}_{3/2u}$
12	1_g	34665	34505	34555	3_g	36552	36744	*35903*	3_g	35930	97% $\pi_{3/2u}f^{\delta}_{3/2u}$
13	4_g	35654	35515	35564	2_u	*36784*	*36995*	36024	2_u	36074	70% $\sigma_{1/2\ g}f^{\delta}_{3/2u}$ + 25% $\sigma_{1/2\ g}f^{\phi}_{5/2u}$
14	3_g	35916	35939	35988	0_g^+	*36693*	*36883*	36141	0_g^+	36115	92% $\pi_{3/2u}f^{\delta}_{3/2u}$
15	2_g	36153	36155	36147	1_u	37140	37344	36393	1_u	36434	93% $\sigma_{1/2\ g}f^{\delta}_{3/2u}$
16	0_g^-	36160	36163	36210	2_u	37302	37525	36472	2_u	36528	69% $\sigma_{1/2\ g}f^{\phi}_{5/2u}$ + 28% $\sigma_{1/2g}f^{\delta}_{3/2u}$
17	0_g^+	36409	36437	36483	3_u	37461	37686	36603	3_u	36669	97% $\sigma_{1/2g}f^{\phi}_{5/2u}$

excited states by taking the first excited state ($^3\Delta_g$) as the reference level, as shown under ΔE^1 in Table 2. From those numbers, it is clear that the IHFSCC and LR-CCSD results are very much alike, both in terms of energies as in the states ordering with respect to symmetry. The difference between the methods appears to mainly arise from a stronger bias for the ground state in the LR-CCSD framework that leads to a systematic overestimation of the transition energies. Less systematic errors are found in comparison with CASPT2, which yields larger discrepancies in the spacing of the different excited states (reaching a few thousand wave numbers for higher states).

3.3. Vertical Transition Energies Including Spin−Orbit Coupling. While instructive for a comparison with other theoretical work, SF results cannot be compared directly to experiment. In order to do so we will now switch on spin−orbit interactions. In this section we will first discuss the tests done to choose the most suitable "active space" in the SO-IHFSCC calculations. These tests are all presented in Table 3, noting that we shall restrict ourselves to excited states lower than 38 000 cm^{-1} which lie well within the accurate P_m model space. Apart from the inherently more difficult theoretical description of higher excited states, we also note that these states form a very dense part of the spectrum, corresponding to the strong absorption broadband that is difficult to resolve experimentally. Thus, the effort in describing them accurately is of limited use for comparison with experimental work.

3.3.1. Influence of Model P_m and Intermediate P_i Spaces. The effect of adding the 5d shell to either the occupied Q or the P_i spaces was explored with the X2C Hamiltonian and turned out to be relatively unimportant (columns 3 to 5 in Table 3). Extending the Q virtual space by including all orbitals with energies $\varepsilon \leq 40.00$ au did also not bring any significant changes to the results relative to the default choice (orbitals up to 20 au). This limits the correlation-active space used in subsequent comparisons to the orbitals with energies between −3 au and 20 au (AS2).

The quality of SO-IHFSCC calculations depends on the partitioning of the correlation space into the main P_m and intermediate P_i spaces. With respect to the creation of valence holes in the occupied orbitals it is possible to extend the minimal P_m space by including the deeper of the two valence occupied $\sigma_{1/2u}$ (see Figure 1 in ref 3) in P_m. Placing this $\sigma_{1/2u}$ in P_m instead of in P_i, shifts the six lowest transition energies up by 1700 cm^{-1} while leaving the other transitions basically unchanged. This significant change favors the inclusion of the deeper $\sigma_{1/2u}$ in the construction of the P_m space. Increasing the P space in the particle space by including all orbitals with energies up to 0.35 au (as opposed to the base value of 0.08 au) has very little effect on the excitation energies but was kept as this extension did not increase calculation times much. The final P_m space is constructed from orbitals with energies between −1.50 and −0.30 au, while the buffering P_i space adds determinants build from holes in the energy ranges [−3.0; −1.50 au] and/or particles in the energy range [−0.30; 0.35 au].

3.3.2. Influence of Hamiltonian and Basis Set Quality. Our results indicate that the X2C method complemented with the atomic mean-field approximation for spin−orbit coupling indeed provides a very good approximation to the DC Hamiltonian, with differences below 200 cm^{-1} upon changing Hamiltonian. This is important in terms of extending the applicability of relativistic methods, as this two-component scheme can yield significant savings in computational time both at the SCF and the 4-index transformation step prior to the correlated calculations. In our calculations, however, computational time was mostly spent in the coupled cluster stage of the calculation, making the choice for the DC approach appropriate. We thus continue at this level and next consider the influence of the basis set choice.

Changing the description of the oxygen atoms from double-ζ quality to triple-ζ hardly affects the eight lowest excitation energies but does have a significant effect on the energies above 31 000 cm^{-1}, with maximal changes of 4000 cm^{-1}. As a

TABLE 4: Equilibrium Geometries (R_e, in Å), Vertical (ΔE^0, in cm^{-1}), and Adiabatic (ΔT_e^0, in cm^{-1}) Spectrum of the Lowest Fine Structure Excited States of UO_2^{2+}, Computed at the SO-IHFSCC, SO-LR-CCSD,[7] and SO-CASPT2[6a]

	SO-IHFSCC[b]					SO-LR-CCSD[c]					SO-CASPT2[d]				
Ω	R_e	ΔE^0	ΔE^1	ΔT_e^0	ΔT_e^1	R_e	ΔE^0	ΔE^1	ΔT_e^0	ΔT_e^1	R_e	ΔE^0	ΔE^1	ΔT_e^0	ΔT_e^1
0_g^+	1.683	0	−18610	0	−17557	1.679	0	−22967	0	−21338	1.708	0	−20104	0	−18888
1_g	1.724	18610	0	17557	0	1.732	22967	0	21338	0	1.765	*20104*	0	*18888*	0
2_g	1.719	18633	23	17834	277	1.743	22789	−178	21826	488	1.782	*19195*	−909	*17227*	−1661
3_g	1.725	19765	1155	18627	1070	1.743	23897	930	22361	1023	1.783	20265	161	18293	−595
2_g	1.722	21080	2470	20082	2525	1.736	25237	2270	24027	2689	1.769	22320	2216	20911	2023
3_g	1.720	23996	5386	23073	5516	1.735	27808	4841	26723	5385	1.769	25435	5331	24026	5138
4_g	1.727	25117	6507	23857	6300	1.743	29054	6087	27923	6585	1.784	26312	6208	24190	5302
3_g	1.730	28132	9522	26679	9122	1.750	32382	9415	30833	9495	1.796	29085	8981	*26446*	7558
2_g	1.731	30230	11620	28757	11200	1.749	34706	11739	*32912*	11574	1.848	31314	11210	*26500*	7612
4_g	1.772	35528	16918	29991	12434	1.798	*39845*	16878	*32113*	10775	1.848	*33262*	13158	*26259*	7371
1_g	1.778	34556	15946	30680	13123	1.795	*39059*	16092	*32815*	11477	1.833	*32921*	12817	27923	9035

[a] Here ΔE^1 and ΔT_e^1 (in cm^{-1}) denote vertical and adiabatic excitations where the origin of the spectrum is taken to be the first excited state. The minima of the SO-IHFSCC calculations (this work) were obtained by extrapolating the symmetrical stretching mode by second-order polynomials. Changes in the ordering of the states are marked in italics. [b] Uranium Fægri and oxygen cc-pVTZ basis sets. [c] Reference 7; uranium ANO-RCC-QZP and oxygen ANO-RCC-TZP basis sets. [d] Reference 6; uranium DK3 and oxygen ANO-L basis sets.

consequence the ordering of states in this energy region changes. Increasing the basis set quality on uranium from double to triple-ζ (Dyall or Faegri types) is again relatively unimportant for the lowest excited states (about 300−500 cm^{-1}), but yield effects of about 1000 cm^{-1} for the higher states. These tests indicate that the triple-ζ basis set size (as used in the spin-free calculations) is indeed a minimal requirement in order to obtain accurate spectroscopic data.

3.3.3. Composition of the Excited States. Having defined a satisfactory computational model (AS2/uranium with a Faegri TZ basis set/oxygen with a cc-VTZ basis set) we may now analyze the influence of spin−orbit coupling on the computed spectrum. The decomposition of the electronic states obtained in the SO-IHFSCC calculations is given in Table 2 in terms of the most significant excited determinants with respect to the ground state. From those numbers it appears that the higher excited states can be described in terms of one main excitation while the eight lowest states have some multireference character. Another interpretation is a difference in spin−orbit induced mixing in these excited states which increases the π-character of the $\sigma_{1/2u}$ orbital relative to the ground state.

The first excited state is sometimes called the luminescent state due to its long lifetime in the 20 000−26 000 cm^{-1} energy range observed in various environments, e.g. in the $Cs_2UO_2Cl_4$ crystal.[68] We calculate this state to be the 1_g state, corresponding to an excitation from the highest $\sigma_{1/2u}$ orbital to the nonbonding $f^{\delta}_{3/2u}$. This is in agreement with spin−orbit configuration interaction results.[4,69] Pierloot et al.[7] and Réal et al.,[7] however, found the 2_g state being the lowest. In all calculations the energy differences between the lowest excited states, and in particular the 1_g and 2_g states, are small (less than 1500 cm^{-1}) and obviously influenced by the quality of the basis sets and electron correlation treatment. All the excitation from the $\sigma_{1/2u}$ to the nonbonding manifolds are located below 31000 cm^{-1}. Above this threshold, the spectrum is dense and almost continuous. The states corresponding to an excitation from the bonding $\pi_{1/2u}$, $\pi_{3/2u}$ orbitals to the nonbonding $f^{\delta}_{3/2u}$, $f^{\delta}_{5/2u}$ and $f^{\phi}_{5/2u}$, $f^{\phi}_{7/2u}$ orbitals are close to the strongly absorbing states, arising from the $\sigma_{1/2g}$ to $f^{\delta}_{3/2u}$, $f^{\delta}_{5/2u}$ and $f^{\phi}_{5/2u}$, $f^{\phi}_{7/2u}$ excitations.

3.4. Excited-State Structures and Comparison between Methods. The potential energy curves along the symmetric stretching vibrational mode relative to the ground-state geometry calculated with the SO-IHFSCC method were investigated and reported in the Table 4. They are displayed in Figure 1. For larger bond distances (>1.75 Å), convergence problems appear in the SO-IHFSCC for the ($1h$,$0p$) sector (which corresponds to calculating the wave functions for ground and excited states of UO_2^{3+}), that could not be remedied by further extending the P_i space. For the two states with an equilibrium bond length above this distance we therefore had to rely on an extrapolation of the curve using a low order polynomial.

The minima of the excited states are reported in the Table 4. All of these U−O_{yl} distances are slightly longer than the ground state distance. States arising from excitations from the bonding $\sigma_{1/2u}$ orbital to the nonbonding $f^{\delta}_{3/2u}$, $f^{\delta}_{5/2u}$ and $f^{\phi}_{5/2u}$, $f^{\phi}_{7/2u}$ have their optimum bond length at about 1.73 Å, while excitations from the $\pi_{1/2u}$, $\pi_{3/2u}$ bonding orbitals (last two states reported in Table 4) yield distances of about 1.78 Å, almost 0.1 Å longer than in the ground state. In general, the SO-IHFSCC bond lengths come close to the SO-LR-CCSD values,[7] about 0.02 Å shorter. This is significantly shorter than the SO-CASPT2 bond lengths, which differ up to 0.06 Å from the SO-IHFSCC values.

Table 4 also contains vertical and adiabatic excitation energies for the three methods in question. Starting with the vertical excitations, for which the comparison between the methods should be more reliable than for the adiabatic energies (again due to the limited precision in the SO-IHFSCC equilibrium geometries), we observe that the SO-IHFSCC transition energies are consistently lower by about 4000 cm^{-1} than the ones computed with SO-LR-CCSD. Like in the scalar relativistic comparison, they come closer to the SO-CASPT2 absolute values, with a difference about 500 cm^{-1} for the 2_g state and up to 2000 cm^{-1} for higher excited states.

The adiabatic transitions computed with the various methods are in line with this picture, but yielding typically one to two thousand wave numbers smaller values for the lower excited states and up to five to six thousand wave numbers for the higher states. It should be noted that the largest differences between vertical and adiabatic energies occur for states with significant Π character ($\pi_{1/2u}$, $\pi_{3/2u} \rightarrow f^{\phi}_{5/2u}$), namely the second 4_g and 1_g states, for which one would indeed expect more significant variations upon geometry changes.

The trends observed here regarding the similarities in the calculated spectra for the three methods are also seen for our spin-free results. This provides a strong indication that the inclusion of spin−orbit coupling a posteriori, as done for LR-CCSD and CASPT2 within one-component frameworks, is quite accurate in this case. As a result, the bulk of the deviations is due to the differences in the correlation treatment, with some smaller contributions from differences in Hamiltonian and/or

basis sets. This is further supported upon inspecting the values of ΔE^1 in Tables 2 and 4, since these clearly show very similar results for SO-IHFSCC (SO a priori) and SO-LR-CCSD (SO a posteriori), and between the spin-free and spin−orbit calculations.

4. Conclusion

In this work we have investigated the performance of three wave function based correlation treatments in the calculation of excitation energies for the uranyl cation. Differences between the two approaches (perturbation theory and coupled cluster), and between different coupled cluster approaches (in particular the linear response and intermediate Hamiltonian Fock-space coupled cluster) are subtle, with comparisons showing similar results from a qualitative perspective but with clear quantitative differences.

The most remarkable quantitative difference between LRCC and IHFSCC is the systematic upward shift of excitation energies in the former, compared to the latter. This shift probably stems from the different parametrization (linear and exponential, respectively) of the wave functions for the excited states in the two coupled cluster methods leading to a larger bias for the ground state in the LRCC calculation. We expect that these discrepancies between LRCC and (IH)FSCC calculations will become smaller with the inclusion of higher excitations within the coupled cluster framework similar to the observations made in work on lighter molecules.

The often-used CASPT2 approach gives a satisfactory agreement with the lowest IHFSCC excitation energies. For higher excitations and relative spacings between excited states the agreement between the two methods larger differences are observed.

The still significant discrepancies between theoretical methods reinforces the call for experimental gas-phase spectroscopic data on the bare uranyl ion to provide a rigorous testing ground for theoretical methods. Direct comparison with experimental data obtained for uranyl crystals or solvated uranyl complexes requires to consider larger chemical models. Work is currently in progress to compute the spectrum of $Cs_2UO_2Cl_4$ using embedding methods, as recently done for the spectrum of NpO_2^{2+} in the $Cs_2UO_2Cl_4$ crystal.[36]

Acknowledgment. We dedicate this article to Prof. R. M. Pitzer, a pioneer in the accurate simulation of actinide spectroscopy. The authors thank Dr. Ivan Infante for providing us information on the relativistic basis sets. This study was supported by a joint project (JRP 06-11) of the EC-supported ACTINET Network of Excellence. F.R. acknowledges a fellowship from the ACTINET network of excellence. Funding was provided by the CNRS and French Ministère de l'Enseignement Supérieur et de la Recherche. Moreover, the authors wish to thank The Netherlands Organization for Scientific Research (NWO) for financial support via the Vici program and acknowledge computer time provided by the Dutch National Computing Facilities (NCF). Additional computational resources have also been provided by the Institut de Développement et de Ressources en Informatique Scientifique du Centre National de la Recherche Scientifique (IDRIS-CNRS) (Contract 71859) and by the Centre Informatique National de l'Enseignement Supérieur, CINES France (Project phl2531).

References and Notes

(1) Denning, R. G. *Struct. Bonding (Berlin)* **1992**, *79*, 215–276.
(2) *The chemistry of the actinide and transactinide elements*; Katz, J. J., Morss, L. R., Fuger, J., Edelstein, N. M., Eds.; Springer-Verlag: Berlin, 2006.
(3) Denning, R. G. *J. Phys. Chem. A* **2007**, *111*, 4125–4143.
(4) Zhang, Z.; Pitzer, R. M. *J. Phys. Chem. A* **1999**, *103*, 6880–6886.
(5) Matsika, S.; Pitzer, R. M. *J. Phys. Chem. A* **2001**, *105*, 637–645.
(6) Pierloot, K.; van Besien, E. *J. Chem. Phys.* **2005**, *123*, 204309.
(7) Réal, F.; Vallet, V.; Marian, C.; Wahlgren, U. *J. Chem. Phys.* **2007**, *127*, 214302.
(8) Wang, Q.; Pitzer, R. M. *J. Phys. Chem. A* **2001**, *105*, 8370–8375.
(9) Pierloot, K.; van Besien, E.; van Lenthe, E.; Baerends, E. J. *J. Chem. Phys.* **2007**, *126*, 194311.
(10) Saue, T.; Fægri, K.; Helgaker, T.; Gropen, O. *Mol. Phys.* **1997**, *91*, 937–950.
(11) Visscher, L.; Saue, T. *J. Chem. Phys.* **2000**, *113*, 3996–4002.
(12) Iliaš, M.; Jensen, H. J. Aa. private communication 2009.
(13) Iliaš, M.; Saue, T. *J. Chem. Phys.* **2007**, *126*, 064102.
(14) Landau, A.; Eliav, E.; Ishikawa, Y.; Kaldor, U. *J. Chem. Phys.* **2000**, *113*, 9905–9910.
(15) Landau, A.; Eliav, E.; Ishikawa, Y.; Kaldor, U. *J. Chem. Phys.* **2001**, *115*, 6862–6865.
(16) Visscher, L.; Eliav, E.; Kaldor, U. *J. Chem. Phys.* **2001**, *115*, 9720–9726.
(17) Eliav, E.; Vilkas, M. J.; Ishikawa, Y.; Kaldor, U. *J. Chem. Phys.* **2005**, *122*, 224113.
(18) Fleig, T.; Olsen, J.; Visscher, L. *J. Chem. Phys.* **2003**, *119*, 2963–2971.
(19) Fleig, T.; Jensen, H. J. Aa.; Olsen, J.; Visscher, L. *J. Chem. Phys.* **2006**, *124*, 104106.
(20) Knecht, S.; Jensen, H. J. Aa.; Fleig, T. 2009, in preparation.
(21) Knecht, S.; Jensen, H. J. Aa.; Fleig, T. *J. Chem. Phys.* **2008**, *128*, 014108.
(22) Szalay, P. G.; Bartlett, R. J. *Chem. Phys. Lett.* **1993**, *214*, 481–488.
(23) Andersson, K.; Malmqvist, P.-Å.; Roos, B. O.; Sadlej, A. J.; Wolinski, K. *J. Phys. Chem.* **1990**, *94*, 5483–5488.
(24) Andersson, K.; Malmqvist, P.-Å.; Roos, B. O. *J. Chem. Phys.* **1992**, *96*, 1218–1226.
(25) Vallet, V.; Maron, L.; Teichteil, C.; Flament, J.-P. *J. Chem. Phys.* **2000**, *113*, 1391–1402.
(26) Christiansen, O.; Hättig, C.; Gauss, J. *J. Chem. Phys.* **1998**, *109*, 4745–4757.
(27) Christiansen, O.; Gauss, J.; Stanton, J. F. *Chem. Phys. Lett.* **1998**, *292*, 437–446.
(28) Christiansen, O.; Gauss, J.; Stanton, J. F. *Chem. Phys. Lett.* **1999**, *305*, 147–155.
(29) Kobayashi, R.; Koch, H.; Jørgensen, P. *Chem. Phys. Lett.* **2002**, *219*, 30–35.
(30) Malmqvist, P.-Å.; Roos, B. O.; Schimmelpfennig, B. *Chem. Phys. Lett.* **2002**, *357*, 230–240.
(31) Llusar, R.; Casarrubios, M.; Barandiarán, Z.; Seijo, L. *J. Chem. Phys.* **1996**, *105*, 5321–5330.
(32) Bast, R.; Jensen, H. J. Aa.; Saue, T. *Int. J. Quantum Chem.* **2009**, *109*, 2091–2112.
(33) Görller-Walrand, C.; De Houwer, S.; Fluyt, L.; Binnemans, K. *Phys. Chem. Chem. Phys.* **2004**, *6*, 3292–3298.
(34) Infante, I.; Gomes, A. S. P.; Visscher, L. *J. Chem. Phys.* **2006**, *125*, 074301.
(35) Infante, I.; Eliav, E.; Vilkas, M. J.; Ishikawa, Y.; Kaldor, U.; Visscher, L. *J. Chem. Phys.* **2007**, *127*, 124308.
(36) Gomes, A. S. P.; Jacob, C. R.; Visscher, L. *Phys. Chem. Chem. Phys.* **2008**, *10*, 5353–5362.
(37) Ruipérez, F.; Danilo, C.; Réal, F.; Flament, J.-P.; Vallet, V.; Wahlgren, U. *J. Phys. Chem. A* **2009**, *113*, 1420–1428.
(38) DIRAC, a relativistic ab initio electronic structure program, Release DIRAC08 (2008), written by Visscher, L.; Jensen, H. J. Aa.; Saue, T. with new contributions from Bast, R.; Dubillard, S.; Dyall, K. G.; Ekström, U.; Eliav, E.; Fleig, T.; Gomes, A. S. P.; Helgaker, T. U.; Henriksson, J.; Iliaš, M.; Jacob, Ch. R.; Knecht, S.; Norman, P.; Olsen, J.; Pernpointner, M.; Ruud, K.; Sałek, P.; Sikkema J. (see http://dirac.chem.sdu.dk).
(39) Dyall, K. G. *J. Chem. Phys.* **1994**, *100*, 2118–2127.
(40) Visscher, L. *Theor. Chem. Acc.* **1997**, *98*, 68–70.
(41) *Program Amfi*, Schimmelpfennig, B., Stockholm University, Sweden.
(42) Heβ, B. A.; Marian, C. M.; Wahlgren, U.; Gropen, O. *Chem. Phys. Lett.* **1996**, *251*, 365–371.
(43) Dyall, K. *Theor. Chem. Acc.* **2007**, *117*, 491–500.
(44) Fægri, K. *Chem. Phys.* **2005**, *311*, 25–34.
(45) Dunning, T. H., Jr. *J. Chem. Phys.* **1989**, *90*, 1007–1023.
(46) Visscher, L.; Dyall, K.; Lee, T. J. *Int. J. Quantum Chem.: Quant. Chem. Symp.* **1995**, *29*, 411–419.
(47) Visscher, L.; Lee, T. J.; Dyall, K. G. *J. Chem. Phys.* **1996**, *105*, 8769–8776.
(48) Pernpointner, M.; Visscher, L.; de Jong, W. A.; Broer, R. *J. Comput. Chem.* **2000**, *21*, 1176–1186.

(49) Pernpointner, M.; Visscher, L. *J. Comput. Chem.* **2003**, *24*, 754–759.
(50) Landau, A.; Eliav, E.; Ishikawa, Y.; Kaldor, U. *J. Chem. Phys.* **2004**, *121*, 6634–6639.
(51) Kaldor, U.; Eliav, E.; Landau, A. Study of Heavy Elements by Relativistic Fock Space and Intermediate Hamiltonian Coupled Cluster Methods. *In Fundamental World of Quantum Chemistry*; Brandas, E. J., Kryachko, E. S., Eds.; Kluwer: Dordrecht, 2004; Vol. 3, pp 365−406.
(52) DALTON, a molecular electronic structure program, Release 2.0 (2005), see http://www.kjemi.uio.no/software/dalton/dalton.html.
(53) Douglas, M.; Kroll, N. M. *Ann. Phys.* **1974**, *82*, 89–155.
(54) Heβ, B. A. *Phys. Rev. A* **1986**, *33*, 3742–3748.
(55) (a) de Jong, W. A.; Visscher, L.; Nieuwpoort, W. C. *J. Mol. Struct. (THEOCHEM)* **1999**, *458*, 41–52. (b) de Jong, W. A.; Visscher, L.; Nieuwpoort, W. C. *J. Mol. Struct. (THEOCHEM)* **2002**, *581*, 259–259.
(56) Straka, M.; Dyall, K. G.; Pyykkö, P. *Theor. Chem. Acc.* **2001**, *106*, 393–403.
(57) Ismail, N.; Heully, J.-L.; Saue, T.; Daudey, J.-P.; Marsden, C. J. *Chem. Phys. Lett.* **1999**, *300*, 296–302.
(58) Garciá-Hernández, M.; Lauterbach, C.; Krüger, S.; Matveev, A.; Rösch, N. *J. Comput. Chem.* **2002**, *23*, 834–846.
(59) Fromager, E.; Réal, F.; Wåhlin, P.; Jenssen, H. J. A.; Wahlgren, U. *J. Chem. Phys.* **2009**, accepted.
(60) Meissner, L.; Bartlett, R. J. *J. Chem. Phys.* **1991**, *94*, 6670−6676.
(61) Meissner, L.; Bartlett, R. J. *J. Chem. Phys.* **1995**, *102*, 7490−7498.
(62) Bartlett, R. J.; Musiał, M. *Rev. Mod. Phys.* **2007**, *79*, 291–352.
(63) Mukhopadhyay, D.; Mukhopadhyay, S.; Chaudhuri, R.; Mukherjee, D. *Theor. Chim. Acta* **1991**, *80*, 441–467.
(64) Helgaker, T.; Jørgensen, P.; Olsen, J. *Molecular Electronic Structure Theory*; John Wiley & Sons: Chichester, 2000.
(65) Musiał, M.; Bartlett, R. J. *J. Chem. Phys.* **2008**, *129*, 044101.
(66) Musiał, M.; Bartlett, R. J. *J. Chem. Phys.* **2008**, *129*, 134105.
(67) Musiał, M.; Bartlett, R. J. *Chem. Phys. Lett.* **2008**, *457*, 267−270.
(68) Denning, R. G.; Snellgrove, T. R.; Woodwark, D. R. *Mol. Phys.* **1976**, *32*, 419–442.
(69) Matsika, S.; Zhang, Z.; Brozell, S. R.; Blaudeau, J.-P.; Wang, Q.; Pitzer, R. M. *J. Phys. Chem. A* **2001**, *105*, 3825–3838.

JP903758C